Oscillations of the ferromagnetic resonance linewidth and magnetic phases in Co/Ru superlattices

W. Alayo and E. Baggio-Saitovitch
Centro Brasileiro de Pesquisas Físicas, Rio de Janeiro 22290-180, Brazil

F. Pelegrini
Instituto de Física, Universidade Federal de Goiás, Goiânia 74001-970, Brazil

V. P. Nascimento
Centro Universitário Norte do Espírito Santo, Universidade Federal do Espírito Santo, São Mateus 29933-415, Brazil

(Received 5 November 2007; revised manuscript received 27 August 2008; published 22 October 2008)

The interlayer exchange coupling (IEC) and the magnetic anisotropy of Co/Ru(0002) *hcp* superlattices, produced by magnetron sputtering, were studied by ferromagnetic resonance (FMR). The main mode and a secondary mode, with a higher resonance field, were identified in the perpendicular FMR spectra. The secondary mode is attributed to the resonance of the bulk of Co magnetic layers while the main mode is associated with the Co/Ru interfacial phase. The linewidth dependence of the main FMR mode on the Ru thickness clearly reproduces the oscillations of the IEC between Co layers. These oscillations are attributed to the effects of lateral inhomogeneities of the IEC strength and have a period of about 12 Å. Moreover, they are in good agreement with magnetoresistance and magnetization measurements performed in the same samples. The dependence of the effective anisotropy constants on the Co layer thickness leads to the volume and surface anisotropy constants of $K_V=-1.10\times10^7$ erg/cm^3 and $2K_s=0.95$ erg/cm^2, respectively, and also to a critical Co thickness of approximately 9 Å below which the magnetization is oriented perpendicular to the plane of the film.

DOI: 10.1103/PhysRevB.78.134417 PACS number(s): 75.30.Gw, 73.21.Cd, 73.21.Ac, 75.30.Ds

I. INTRODUCTION

Magnetic multilayers are a subject of intense research due to their rich magnetic properties and potential applications in magnetoresistive and spintronics devices. The giant magnetoresistance,[1] the interlayer exchange coupling, and the magnetic anisotropy are some of the most important features of magnetic multilayers. The discovery of the interlayer exchange coupling (IEC), which oscillates between ferromagnetic (FM) and antiferromagnetic (AF) as a function of the spacer layer thickness,[2] has led to an increased interest in the topic of magnetic multilayers. The most prominent approaches to explain the oscillatory behavior of the IEC include the Ruderman-Kittel-Kasuya-Yosida[3–5] and the quantum-well models,[6–8] which are based on the response of the conduction electrons of the spacer material separating the magnetic layers. On the other hand, the magnetic anisotropy is due to various mechanisms, including shape and magnetocrystalline anisotropies, magnetostriction, and the reduced symmetries at the interfaces. The interface-induced anisotropy is strongly dependent on the preparation techniques and conditions. A recent review of IEC and magnetic anisotropy in thin films can be found in a recent book by Burstein *et al.*[9]

Co/Ru multilayers particularly are good prototypes to investigate the magnetism of thin films. The IEC in this system has been observed and investigated by several groups with different techniques.[2,10–13] However, there are no reports focusing on the oscillations of the IEC from the point of view of the ferromagnetic resonance (FMR) linewidth in the Co/Ru system. The linewidth is one of the most sensitive parameters in FMR and it can be affected by the exchange interaction. In the FMR of exchange-coupled multilayers, the interlayer exchange is considered as an additional torque acting on the surface spins of each magnetic layer and it can be represented by an effective field and included in the Landau-Lifshitz-Gilbert equation of motion. This exchange field leads to an inhomogeneous broadening of the line as the spacer thickness increases.[14,15] Variations in the spacer thickness are also accompanied by roughness changes, leading to small lateral variations of the exchange field.[14] These lateral variations can be understood as a lateral inhomogeneity of the IEC strength, which affects the linewidth in FMR. This effect scales with the IEC and thus, oscillations of the linewidth as a function of the spacer thickness may be understood as oscillations of the IEC.[14,16,17] Here, the FMR measurements in Co/Ru superlattices show that the dependence of the FMR linewidth of the main mode on the thickness of the Ru spacer reflects the oscillations of the IEC.

In the FMR spectra of several Co-based multilayers, an additional resonance mode, which is not due to the exchange interaction and whose origin is still unclear, has been observed. As examples we have the Co/Pt,[18] Co/Au,[19] and Co/Pd (Refs. 20 and 21) multilayers. In the studies reported here, an additional mode was also observed, with a resonance field higher than the resonance field of the main mode in the perpendicular configuration of the applied external field. The origin of this mode in Co/Ru multilayers has not been discussed before and here an interpretation based on x-ray diffraction results is proposed. A study of the magnetic anisotropy of the Co/Ru superlattices was also performed, giving the interface and volume contributions to the magnetic anisotropy energy and the critical Co layer thickness below which the magnetization is preferentially oriented perpendicular to the film plane.

II. PHENOMENOLOGICAL DESCRIPTION OF FMR AND CONTRIBUTIONS TO THE LINEWIDTH

For a description of FMR in thin films, the following coordinate system was considered: The film surface is in the x-y plane, the external magnetic-field vector ($\vec{H}$) forms the θ_H angle with respect to the normal to the film plane (z axis), and the direction of the magnetization ($\vec{M}$) of the film is defined by the azimuthal φ and polar θ angles. The external microwave field is perpendicular to the applied field $\vec{H}$. When the film is in the presence of $\vec{H}$, $\vec{M}$ interacts with an effective magnetic field, given by $\vec{H}_{\text{eff}}=\vec{H}+\vec{H}_{\text{int}}$, where $\vec{H}_{\text{int}}$ represents the internal fields of the sample. The precession of $\vec{M}$ is around $\vec{H}_{\text{eff}}$ and it is described by the Landau-Lifshitz-Gilbert equation of motion:[22]

$$\frac{d\vec{M}}{dt} = -\gamma\vec{M}\times\vec{H}_{\text{eff}} + \frac{G}{\gamma M_s^2}\vec{M}\times\frac{\partial\vec{M}}{\partial t}, \tag{1}$$

where $\gamma=g\mu_B/\hbar$ is the gyromagnetic ratio, g is the Landé factor, μ_B is the Bohr magneton, G is the Gilbert-damping parameter, and M_s is the saturation magnetization of the film. Neglecting the damping effect in Eq. (1), the equilibrium and resonance conditions can be written, respectively, as

$$H_r\cos(\theta-\theta_H) = 4\pi M_{\text{eff}}\sin\theta\cos\theta \tag{2}$$

and

$$(\omega/\gamma)^2 = [H_r\cos(\theta-\theta_H) - 4\pi M_{\text{eff}}\cos^2\theta] \times[H_r\cos(\theta-\theta_H) - 4\pi M_{\text{eff}}\cos 2\theta]. \tag{3}$$

Here an effective magnetization is defined as $4\pi M_{\text{eff}} = 4\pi M_s - H_k$, where H_k is the perpendicular anisotropy field. The contributions to the free energy of the films considered here are the Zeeman energy, demagnetizing energy, and first-order anisotropy energy. Equations (2) and (3) were used to calculate the anisotropy constants of the Co/Ru superlattices.

The enhancement of the magnetization damping which is due to the inhomogeneity of the IEC and its effect upon the FMR linewidth, takes into account of the fact that the basic contributions to the FMR linewidth can be written as[23]

$$\Delta H = \Delta H_{\text{hom}} + \Delta H_{\text{inhom}}, \tag{4}$$

where ΔH_{hom} describes the intrinsic mechanism of relaxation in terms of the Gilbert-damping parameter and the saturation magnetization, and ΔH_{inhom} describes an inhomogeneous broadening due to sample defects. This inhomogeneous broadening is due to the spread in the orientation of the crystallographic axes and variations of the internal magnetic fields ΔH_{int} throughout the sample. ΔH_{int} makes its most significant contribution to the linewidth as the magnetization approaches the orientation normal to the film. Since ΔH_{int} is related to the interlayer exchange by an effective exchange field, the total linewidth may be affected by an inhomogeneous broadening coming from variations in the spacer roughnesses, which consequently produce a small lateral variation in the coupling field. Another mechanism which can also contribute to the ΔH_{inhom} term in multilayers is the two-magnon scattering of defects on the film surfaces.[23,24] However, this mechanism becomes inactive when the magnetization approaches the normal to the film plane.

III. EXPERIMENTAL DETAILS

The Co/Ru superlattices studied in this work were prepared at room temperature with a dc-magnetron sputtering system. They were deposited onto a Ru(50 Å) buffer layer over Si(100) single-crystal substrates and covered by a protective Ta(50 Å) cap layer. The base pressure of the deposition chamber was less than 5×10^{-8} Torr and the Ar pressure (working pressure) was kept constant at 2×10^{-3} Torr. The deposition rates of both Co and Ru were of the order of 1 Å/s. The samples were prepared with Ru thicknesses varying between 9 and 33 Å and Co thicknesses between 10 and 50 Å, which implies that the total thickness of the samples varied between approximately 880 and 1100 Å.

The structural properties of the samples were analyzed by x-ray reflectivity and x-ray diffraction. The data were taken with a standard $\theta-2\theta$ diffractometer, using the K_α radiation of Cu. Magnetoresistance versus magnetic-field measurements were performed using the four point method, with the current in-plane (CIP) geometry, where the current is applied in the plane of the films with the magnetic field also in the film plane, but perpendicular to the current. Magnetization measurements were obtained with a superconducting quantum interference device magnetometer, with the magnetic field applied parallel to the sample plane.

The FMR experiments were performed using a high sensitive Bruker ESP-300 spectrometer operating at the X-band microwave frequency (9.79 GHz) and swept static magnetic field. The FMR spectra were taken using standard modulation and phase-sensitive detection techniques with the film at the center of a high-Q rectangular resonant cavity. All the experiments, i.e., structural characterization, magnetoresistance, magnetization, and FMR were performed at room temperature.

IV. RESULTS AND DISCUSSION

A. Structural characterization

Representative x-ray reflectivity and x-ray diffraction results are shown in Fig. 1 for a $[\text{Co}(50\ \text{Å})/\text{Ru}(15\ \text{Å})]_{20}$ superlattice. In the reflectivity pattern [Fig. 1(a)], up to six Bragg peaks, due to the chemical modulation, are clearly visible, confirming the periodic layered structure of our samples. The period calculated from the positions of the peaks ($\Lambda=63$ Å) is very close to the nominal value ($\Lambda=65$ Å), i.e., there is a difference of about 3% between the nominal and calculated values. The combination of sharp diffraction features with up to sixth order reflections indicates that the layers are smooth and have well-formed interfaces. The interfacial roughness was estimated to be about 7 Å (mean-square roughness) by fitting the x-ray reflectivity curves using the Phillips WINGIXA refinement program. The high-angle diffractogram is shown in Fig. 1(b), with the main Bragg peak located at $2\theta=43.7°$ which corresponds to a Co/Ru (0002) *hcp* structure. Several satellite peaks are also present, which is a signature of a well-defined multilayered

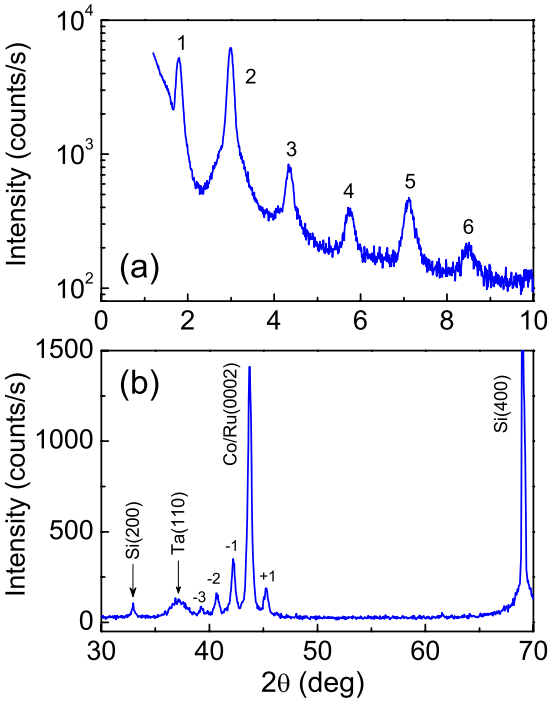

FIG. 1. (Color online) (a) X-ray reflectivity and (b) x-ray diffraction patterns of the $[Co(50\ Å)/Ru(15\ Å)]_{20}$ sample.

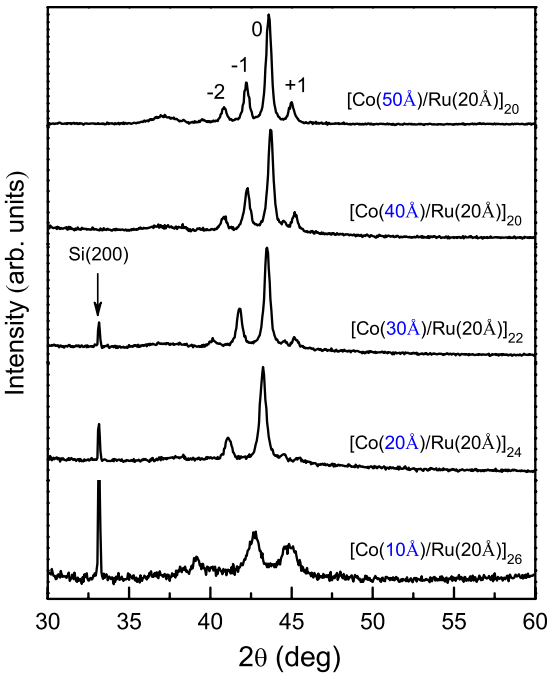

FIG. 2. (Color online) X-ray diffraction patterns of Co/Ru superlattices with a constant (20 Å) Ru layer thickness and several Co layer thicknesses.

structure, indicating a good stacking of the layers and confirming the good quality of the samples. The grain size, calculated from the linewidth at the half-height of the main peak by using the Scherrer formula,[25] is around 225 Å, i.e., four bilayers are coherent in the growth direction. The Si(400) peak of the substrate and the Ta(110) peak of the capping layer can also be identified.

The x-ray diffraction results for samples with different Co layer thicknesses and 20 Å of Ru are shown in Fig. 2. It can be seen that the crystalline quality is gradually reduced when the Co layer thickness decreases. The grain sizes (ξ), calculated with Scherrer formula, are summarized in Table I, where an increment of ξ with the Co layer thickness can be observed. For samples with the same Co layer thickness (50 Å) and different Ru thicknesses (varying from 9 to 33 Å), grain sizes between 210 and 225 Å were found.

B. Magnetization and magnetoresistance measurements

To show evidences of an oscillatory IEC in our Co/Ru samples, measurements of magnetization and magnetoresistance as a function of the applied magnetic field were performed in multilayers with different Ru thicknesses. Results and comments are presented below.

Normalized hysteresis loops of $[Co(50\ Å)/Ru(t_{Ru})]_{20}$ superlattices with $t_{Ru}=11$, 15, 17, and 20 Å are shown in Fig. 3(a). The loops were measured along the plane of the films and the magnetization per unit volume, as expected, is independent of the Ru thickness. However, the shape of the curves depends on the thickness of the Ru spacer, which determines the magnetic coupling between Co layers. The saturation fields for samples with $t_{Ru}=15$ and 17 Å are much larger than those with $t_{Ru}=11$ and 20 Å. The dependence of the saturation field on the Ru thickness is shown in Fig. 3(b), where two oscillations can be seen with a period of approximately 12 Å. The two maxima observed in Fig. 3(b) occur at $t_{Ru}=17$ and 30 Å with saturation fields of 1470 and 800 Oe, respectively, and are in good agreement with those reported by Parkin *et al.*[2] for Co/Ru superlattices produced by sputtering on Si(111) wafers. The dependence of the maximum magnetoresistance (MR) on the Ru thickness of the same multilayer system is shown in Fig. 3(c). The MR values are low, but the oscillatory dependence with t_{Ru} can be clearly observed and the oscillations have the same period of 12 Å as found in the analysis of the magnetization curves. The maxima also occur at $t_{Ru}=17$ and 30 Å with MR values of 1.14 and 0.8%, respectively. The oscillations of the saturation field and of the magnetoresistance as a function of the Ru spacer thickness show clear changes in the sign of the IEC of the Co/Ru multilayers. The Co layers are antiparallel coupled in the ranges of 15–17 Å and 29–31 Å of Ru thickness. The H_s and MR values in the first antiferromagnetic range are larger than those of the second one, providing

TABLE I. Grain sizes (ξ) of Co/Ru superlattices with different Co layer thicknesses, obtained from the x-ray diffraction analysis.

Sample	Grain size ξ (Å)
$[Co(10\ Å)/Ru(20\ Å)]_{26}$	85
$[Co(20\ Å)/Ru(20\ Å)]_{24}$	184
$[Co(30\ Å)/Ru(20\ Å)]_{22}$	208
$[Co(40\ Å)/Ru(20\ Å)]_{20}$	225
$[Co(50\ Å)/Ru(20\ Å)]_{20}$	225

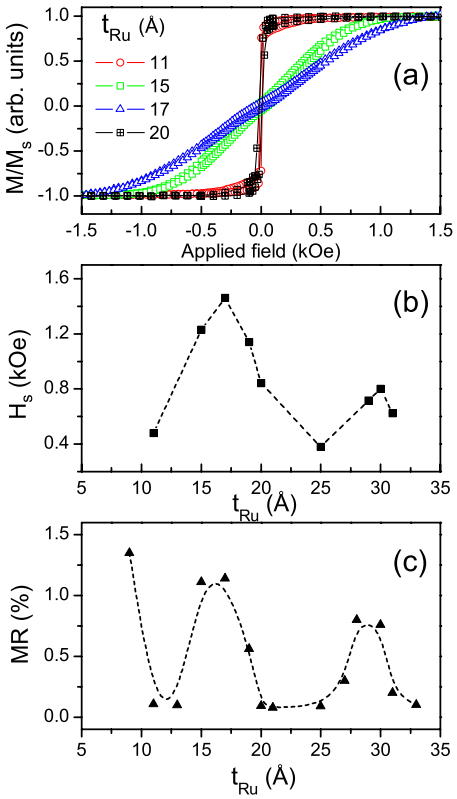

FIG. 3. (Color online) (a) Normalized hysteresis loops of the $[\mathrm{Co}(50\ \text{Å})/\mathrm{Ru}(t_{\mathrm{Ru}})]_{20}$ superlattices for $t_{\mathrm{Ru}}=11$, 15, 17, and 20 Å, measured at room temperature and with magnetic field along the film plane. (b) Dependence of the in-plane saturation field on the Ru thickness. (c) Dependence of the CIP magnetoresistance on the Ru thickness.

additional evidence that the coupling strength decreases with the Ru thickness.

C. Analysis by ferromagnetic resonance

Representative FMR spectra for Co/Ru superlattices are shown in Fig. 4. They correspond to the $[\mathrm{Co}(50\ \text{Å})/\mathrm{Ru}(17\ \text{Å})]_{20}$ sample, giving evidence of a main mode and a secondary higher field mode in the perpendicular configuration ($\theta_H=0°$ between the applied magnetic field and the normal to the film plane). With increasing θ_H, the resonance field for both modes decreases. At a specific angle θ_H of approximately 9°, the two modes cross each other. With a further increase of θ_H, the two modes separate again and in the parallel configuration ($\theta_H=90°$), the resonance field of the main mode is larger than that of the secondary mode. The out-of-plane angular dependence of the absorption fields for both main and secondary FMR modes of the $[\mathrm{Co}(50\ \text{Å})/\mathrm{Ru}(17\ \text{Å})]_{20}$ superlattice is shown in Fig. 5. Open triangles represent the experimental data and the dashed lines are results from fits performed with the equilibrium and resonance conditions, given by Eqs. (2) and (3). The inset in Fig. 5 shows the calculated slope of the H_r versus θ_H curve for the main mode. These fits give $4\pi M_{\mathrm{eff}}=13.07$ kOe and $g=2.0$ for the main mode and $4\pi M_{\mathrm{eff}}=14.25$ kOe and $g=2.1$ for the secondary mode. These values are lower than the known values[26] of $4\pi M_{\mathrm{eff}}=17.80$ kOe and $g=2.22$ of bulk Co. This may imply that both magnetic phases could be Co-Ru alloys with different Ru content, as it was also observed in magnetron sputtered Co/V multilayers[27] with two uniform FMR absorption modes attributed to bulk and interfacial phases. Two uniform FMR modes observed in the spectra of pure Co monolayer films deposited by evaporation on Si and glass substrates[28] were also attributed to different magnetic phases in the samples. The first one was attributed to the region of the Co layer near the substrate, and the second one, to the free region of the Co layer. The second FMR mode, with a higher resonance field, increases in amplitude and becomes more intense than the first one, with a lower resonance field, as the thickness of the Co layer is increased.

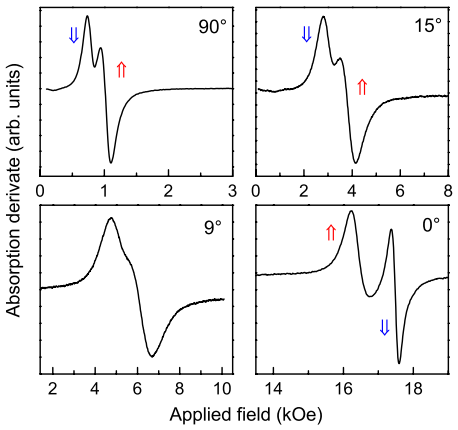

FIG. 4. (Color online) FMR spectra of the $[\mathrm{Co}(50\ \text{Å})/\mathrm{Ru}(17\ \text{Å})]_{20}$ sample for some orientations between the external magnetic field and the normal to the film plane. (⇑) Main uniform mode, (⇓) secondary mode.

The FMR spectra measured with $\theta_H=0°$ in samples with different Co layer thicknesses and a constant (20 Å) thickness of Ru layers are shown in Fig. 6. For $t_{\mathrm{Co}}=10$ and 20 Å,

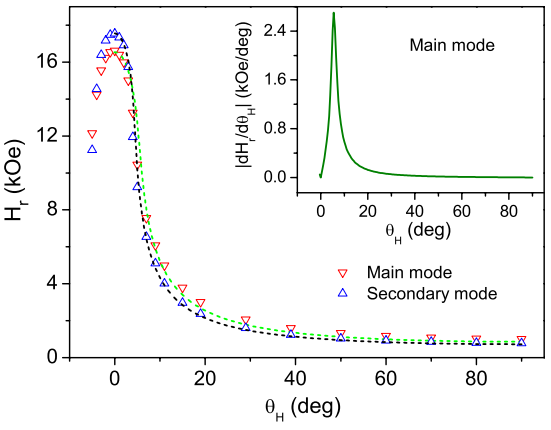

FIG. 5. (Color online) Out-of-plane angular dependence of the resonance field of the two FMR modes of the $[\mathrm{Co}(50\ \text{Å})/\mathrm{Ru}(17\ \text{Å})]_{20}$ sample. Open triangles are the experimental results and dashed lines are fits performed with Eqs. (2) and (3). The inset is the calculated slope of the H_r versus θ_H curve for the main mode.

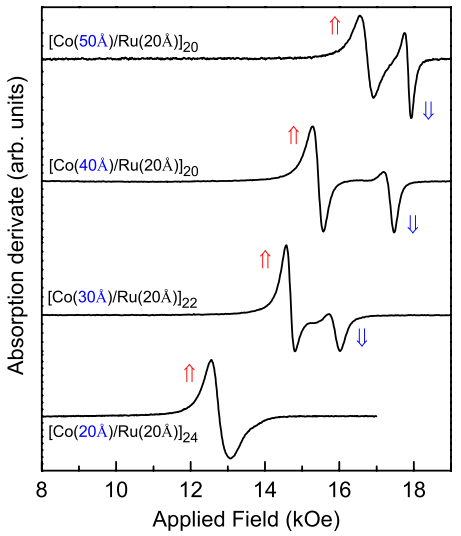

FIG. 6. (Color online) Perpendicular FMR spectra of Co/Ru superlattices with different Co layer thicknesses. (⇑) Main uniform mode, (⇓) secondary mode.

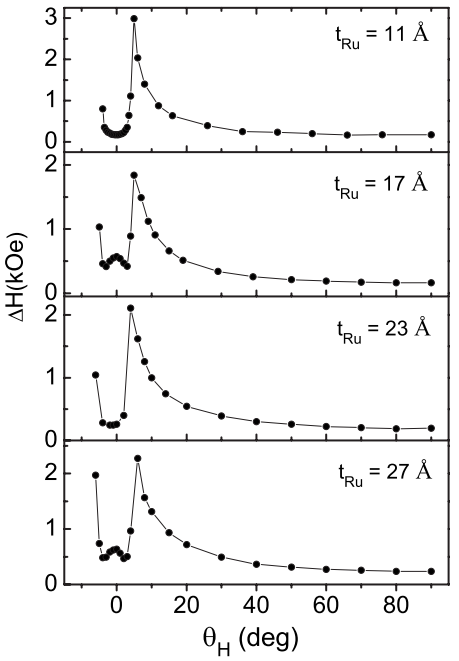

FIG. 7. Out-of-plane angular dependence of the linewidth of the main FMR mode of the $[\mathrm{Co}(50\ \text{Å})/\mathrm{Ru}(t_{\mathrm{Ru}})]_{20}$ superlattices for $t_{\mathrm{Ru}}=11$, 17, 23, and 27 Å. Solid lines are just guides for the eyes.

only the main mode was excited by the microwave field; the spectrum for $t_{\mathrm{Co}}=10$ Å is wider and it is not shown here. The observation of two well-defined resonance modes, in the spectra shown in Figs. 5 and 6, suggests the presence of two magnetic regions in the samples. For $t_{\mathrm{Co}}=10$ and 20 Å only one mode is observed due to only one magnetic phase present. As t_{Co} increases to 30 Å the secondary mode appears and becomes more intense with increasing t_{Co}, suggesting the formation of a second magnetic phase that increases in volume with t_{Co} (the intensity of the mode is proportional to the magnetization times the volume of the region). We believe that the first magnetic phase, giving the main FMR mode, excited by the microwave field in all samples, corresponds to Co/Ru interfacial regions with a lower effective magnetization. The second magnetic phase, giving the secondary FMR mode, is believed to be associated with the bulk of the Co layers with a higher effective magnetization. FMR measurements in the parallel geometry of the applied field support this conclusion. The spectra showed two absorption modes (clearly separated for samples with thick Co layers) and give evidence of hard and easy magnetization axes in the plane of the films, 90° apart and with an anisotropy field of up to 40 Oe. The reduced $4\pi M_{\mathrm{eff}}$ value of the main FMR mode, attributed to the Co/Ru interfacial regions, could also be due to an induced spin polarization of Ru. It is known in the literature[29] that Ru polarizes when in contact with Co. This spin polarization can lead to a reduction of Co magnetic moments at the Co/Ru interfaces and consequently of the effective magnetization, forming a region with a lower effective magnetization as a distinct phase in the sample. However, the possibility of the Ru polarization and the reduction of Co magnetic moments, as well as other interface effects, need to be analyzed in more detail with element-selective techniques.

The reduction of the resonance fields of both the resonance modes in Fig. 6, as the Co layer thickness is decreased, is an indication of a decrease of the local effective magnetization. This can be better understood if we consider the resonance condition for a magnetic field applied perpendicular to the plane of the film, given by[14] $\omega/\gamma=H_r-4\pi M_{\mathrm{eff}}$. In the FMR experiments performed here, the microwave angular frequency ω was kept constant and the γ factor is considered as a constant of the material. Thus, a reduction of the local effective magnetization $4\pi M_{\mathrm{eff}}$ results in a decrease of the resonance field H_r in the perpendicular FMR spectra. This reduction of $4\pi M_{\mathrm{eff}}$ is due to surface and interface effects. For the Co layer thicknesses in the ranges used here (50–10 Å), the surface and interface effects strongly affect the effective local magnetization, since the contribution of the spin-orbit interaction to the free energy starts to overcome the contribution of the dipole-dipole interaction. For larger Co thicknesses, variations of H_r are negligible since at these thicknesses the bulk effects overcome the surface and interface effects.

In order to see an inhomogeneous broadening of the linewidth, the total peak to peak linewidth was measured as a function of the out-of-plane angle. The inhomogeneous contribution to the total linewidth arises from the broadening induced by magnetic inhomogeneities, such as the internal static magnetic fields and the orientation of the crystallographic axis or anisotropy axis. This contribution should always be considered in magnetic multilayers, since all multilayer samples have defects that can give rise to magnetic inhomogeneities. Figure 7 shows the ΔH versus θ_H curves of the main FMR mode of the $[\mathrm{Co}(50\ \text{Å})/\mathrm{Ru}(t_{\mathrm{Ru}})]_{20}$ superlattices for $t_{\mathrm{Ru}}=11$, 17, 23, and 27 Å. The shape of the curves implies that the linewidth is composed of a homogeneous and an inhomogeneous parts. The homogeneous part is due to an intrinsic damping mechanism that is always present in the samples, whereas the inhomogeneous part is usually written as[23]

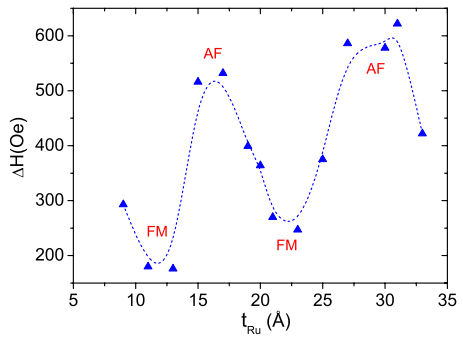

FIG. 8. (Color online) Dependence of the linewidth of the main mode of the perpendicular FMR spectra on the Ru layer thickness of the $[\mathrm{Co}(50\ \text{Å})/\mathrm{Ru}(t_{\mathrm{Ru}})]_{20}$ superlattices. The dashed line is just a guide for the eyes.

$$\Delta H_{\mathrm{inhom}} = \left|\frac{\partial H_r}{\partial \theta_H}\right| \Delta\theta_H + \left|\frac{\partial H_r}{\partial \phi_H}\right| \Delta\phi_H + \left|\frac{\partial H_r}{\partial H_{\mathrm{int}}}\right| \Delta H_{\mathrm{int}}, \tag{5}$$

where $\Delta\theta_H$ and $\Delta\phi_H$ represent the spread in the orientation of the crystallographic axes and ΔH_{int} represents the variations of the internal magnetic fields throughout the sample. The sharp peaks of the curves in Fig. 7 are given by the slope of the respective H_r versus θ_H curves and it is described by the $|\partial H_r/\partial\theta_H|\Delta\theta_H$ term in Eq. (5), as shown by the inset of Fig. 5 for the main mode of the $[\mathrm{Co}(50\ \text{Å})/\mathrm{Ru}(17\ \text{Å})]_{20}$ superlattice. In this work, no simulations of the linewidth were performed. The experimental results just give evidence that the linewidth of the main FMR mode in the perpendicular configuration of the applied field has an oscillatory dependence with the Ru layer thickness, following the same behavior of the IEC. In Fig. 8, this dependence is shown for the $[\mathrm{Co}(50\ \text{Å})/\mathrm{Ru}(t_{\mathrm{Ru}})]_{20}$ superlattices, which were also analyzed by magnetoresistance and magnetization measurements. The period of the oscillations is also 12 Å and the two maxima occur in the same ranges of Ru thicknesses deduced from the dependence of the H_s and MR values on the Ru thickness, shown in Figs. 3(b) and 3(c), respectively. Furthermore, a broadening of the linewidth of about 400 Oe can be seen from the ferromagnetic to the antiferromagnetic phase. This suggests that the damping process of the magnetization is influenced by contributions coming from the inhomogeneity of the IEC strength. If we assume an ideal case where the Co/Ru interfaces are perfectly flat and the effect of interface roughness is negligible, the separation between Co layers would be homogeneous, i.e., the Ru layer thickness would be the same in different parts of the sample, leading to a homogeneous distribution of the IEC strength throughout the whole sample. But in our case, where interfacial roughnesses are present and play an important role, the separation between Co layers is inhomogeneous in the whole sample. This leads to an inhomogeneous distribution of the IEC strength between magnetic layers. These inhomogeneities of the IEC strength can be treated as variations of the coupling field and consequently of the internal fields and lead to slightly different resonance fields which influence the inhomogeneous part of the linewidth and consequently the total linewidth. This results in a broadening of the total linewidth due to the overlap of the signals coming from different regions of the sample. Indeed, as evidenced by the x-ray diffraction and x-ray reflectivity results, the Co/Ru samples analyzed in this work have good stacking of the layers but the interfaces present roughnesses whose mean-square value was estimated by fitting the reflectivity patterns. These roughnesses are believed to be responsible for the inhomogeneous interlayer exchange coupling. The inhomogeneity of the internal fields is described by the $|\partial H_r/\partial H_{\mathrm{int}}|\Delta H_{\mathrm{int}}$ term in Eq. (5) and represents contributions to the linewidth coming from variations of the resonance field with respect to the internal fields. Moreover, as Fig. 8 reveals, the inhomogeneity of the IEC strength scales with the coupling between Co layers on the Ru thickness, leading to oscillations of the linewidth as a function of t_{Ru}. Oscillations and broadening of the FMR linewidth due to inhomogeneities were also reported in Co/Cu multilayers,[15] Co/Cu superlattices,[16] and NiFe/Ru/NiFe trilayers.[17]

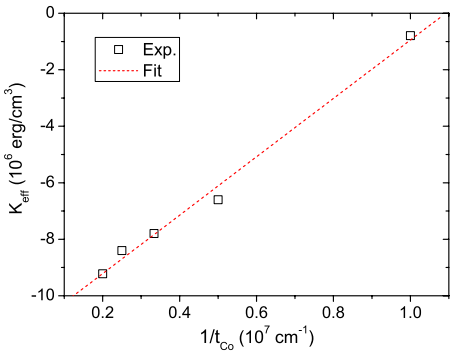

FIG. 9. (Color online) Plot of K_{eff} versus $1/t_{\mathrm{Co}}$ for the $[\mathrm{Co}(t_{\mathrm{Co}})/\mathrm{Ru}(20\ \text{Å})]_{\mathrm{N}}$ superlattices. Open squares are the experimental values and the dashed line is the fit performed with Eq. (6).

Magnetic anisotropy

The interface and volume contributions to the anisotropy energy of Co/Ru superlattices can be obtained by using the anisotropy constant values of samples with different Co layer thicknesses. The effective anisotropy is defined as $K_{\mathrm{eff}}=K_u-2\pi M_s^2$, where M_s is the saturation magnetization and K_u is the anisotropy constant which contains the magnetocrystalline and magnetoelastic contributions. The K_{eff} values can be deduced using $4\pi M_{\mathrm{eff}}=4M_s-2K_u/M_s$, with the effective magnetization values obtained by fitting the out-of-plane angular dependence of the resonance field, as was performed for the $[\mathrm{Co}(50\ \text{Å})/\mathrm{Ru}(17\ \text{Å})]_{20}$ sample. According to the well-known phenomenological model, which relates the effective anisotropy constant to the thickness t of the magnetic layer and the volume K_V and interface K_s anisotropy constants, given by[30]

$$K_{\mathrm{eff}} = K_V + 2K_s/t_{\mathrm{Co}}, \tag{6}$$

the K_V and K_s values can be obtained by fitting K_{eff} as a function of $1/t_{\mathrm{Co}}$. The plot of K_{eff} versus $1/t_{\mathrm{Co}}$ of the Co/Ru superlattices is shown in Fig. 9. Open squares represent the experimental data and the dashed line is the result of a fit

performed using Eq. (6). The fit yields $K_V=-1.10\times10^7$ erg/cm^3, which includes the demagnetization energy and the magnetocrystalline energy, and $2K_s=0.95$ erg/cm^2, which is associated with the Néel anisotropy. Furthermore, we can estimate a critical Co layer thickness (t_c), below which the magnetization should be preferentially oriented perpendicular to the film plane by using $t_c=2K_s/K_V$. The value of t_c is approximately 9 Å. The anisotropy constant values and the critical Co thickness are very close to the known experimental values given in the literature[31] for evaporated Co/Ru(0001) superlattices.

V. SUMMARY AND CONCLUSIONS

In summary, Co/Ru superlattices were grown over Si(100) wafers by dc-magnetron sputtering at room temperature and characterized by x-ray reflectivity, x-ray diffraction, magnetization, magnetoresistance, and ferromagnetic resonance measurements. The samples analyzed in this work have good structural quality and smooth interfaces as evidenced by the x-ray diffraction and x-ray reflectivity analyses. The FMR spectra show two absorption modes, the main mode and a secondary mode with a higher resonance field when the external magnetic field is applied perpendicular to the film plane. These modes were attributed to the presence of two magnetic phases in the samples. The first one, which is located in the main mode and has a lower effective magnetization, is found in the interfacial Co/Ru regions, while the second mode, with a higher effective magnetization, is the bulk of the Co layers. The interfacial roughness leads to an inhomogeneous distribution of the IEC strength. This inhomogeneity leads to a broadening and oscillations of the FMR linewidth as a function of the Ru thickness, reflecting the oscillations of the exchange coupling between Co layers with a period of about 12 Å, between ferromagnetic and antiferromagnetic couplings, also observed with magnetoresistance and magnetization measurements. The values of the effective anisotropy constant (K_{eff}), obtained by fitting the out-of-plane angular dependence of the resonance field of the main mode in samples with different Co layer thicknesses, imply the volume and surface anisotropy constants of $K_V=-1.10\times10^7$ erg/cm^3 and $2K_s=0.95$ erg/cm^2, respectively. They also imply a critical Co thickness of approximately 9 Å below which the magnetization is oriented perpendicular to the film plane.

ACKNOWLEDGMENTS

This work was supported by Brazilian funding agencies CLAF, CNPq, and FAPERJ (Pronex and Cientista do Estado). W.A. also acknowledges the PCI program from CBPF.

[1] M. N. Baibich, J. M. Broto, A. Fert, F. Nguyen Van Dau, F. Petroff, P. Eitenne, G. Creuzet, A. Friederich, and J. Chazelas, Phys. Rev. Lett. **61**, 2472 (1988).
[2] S. S. P. Parkin, N. More, and K. P. Roche, Phys. Rev. Lett. **64**, 2304 (1990).
[3] Y. Yafet, Phys. Rev. B **36**, 3948 (1987).
[4] R. Coehoorn, Phys. Rev. B **44**, 9331 (1991).
[5] P. Bruno and C. Chappert, Phys. Rev. Lett. **67**, 1602 (1991).
[6] D. M. Edwards, J. Mathon, R. B. Muniz, and M. S. Phan, Phys. Rev. Lett. **67**, 493 (1991).
[7] P. Bruno, J. Phys.: Condens. Matter **11**, 9403 (1999).
[8] M. D. Stiles, J. Magn. Magn. Mater. **200**, 322 (1999).
[9] E. Burstein, M. L. Cohen, D. L. Mills, and P. J. Stiles, *Nanomagnetism: Ultrathin Films, Multilayers and Nanostructures (Contemporary Concepts of Condensed Matter)*, 1st ed. (Elsevier, New York, 2006).
[10] K. Ounadjela, D. Muller, A. Dinia, A. Arbaoui, P. Panissod, and G. Suran, Phys. Rev. B **45**, 7768 (1992).
[11] P. J. H. Bloemen, H. W. van Kesteren, H. J. M. Swagten, and W. J. M. de Jonge, Phys. Rev. B **50**, 13505 (1994).
[12] A. Rampe, D. Hartmann, W. Weber, S. Popovic, M. Reese, and G. Guntherodt, Phys. Rev. B **51**, 3230 (1995).
[13] S. Zoll, A. Dinia, J. P. Jay, C. Meny, G. Z. Pan, A. Michel, L. El Chahal, V. Pierron-Bohnes, P. Panissod, and H. A. M. Van den Berg, Phys. Rev. B **57**, 4842 (1998).
[14] J. Lindner and K. Baberschke, J. Phys.: Condens. Matter **15**, R193 (2003).
[15] Q. Y. Jin, H. R. Zhai, Y. B. Xu, Y. Zhai, M. Lu, S. M. Zhou, J. S. Payson, G. L. Dunifer, R. Naik, and G. W. Auner, J. Appl. Phys. **77**, 3971 (1995).
[16] A. L. Kaplienko, E. P. Nikolova, K. V. Kut'ko, A. G. Anders, V. V. Zorchenko, and A. N. Stetsenko, Low Temp. Phys. **31**, 358 (2005).
[17] M. Belmeguenai, T. Martin, G. Woltersdorf, M. Maier, and G. Bayreuther, Phys. Rev. B **76**, 104414 (2007).
[18] J. O. Artman, D. J. DeSmet, X. Shao, J. C. Cates, C. Alexander, Jr., M. R. Parker, E. T. Lacey, D. G. Lord, and P. J. Grundy, J. Appl. Phys. **70**, 6038 (1991).
[19] Peng Chubing, Dai Daosheng, and Fang Ruiyi, Phys. Rev. B **46**, 12022 (1992).
[20] N. A. Lesnik and R. Gontarz, J. Magn. Magn. Mater. **140-144**, 607 (1995).
[21] J. A. Romano, E. C. da Silva, L. F. Schelp, J. E. Schmidt, R. Meckenstock, and J. Pelzl, J. Magn. Magn. Mater. **205**, 161 (1999).
[22] B. Heinrich, *Ultrathin Magnetic Structures II*, 1st ed. (Springer-Verlag, Berlin, 1994), pp. 195–222.
[23] W. Platow, A. N. Anisimov, G. L. Dunifer, M. Farle, and K. Baberschke, Phys. Rev. B **58**, 5611 (1998).
[24] S. J. Yuan, L. Sun, H. Sang, J. Du, and S. M. Zhou, Phys. Rev. B **68**, 134443 (2003).
[25] B. D. Cullity, *Elements of X-Ray Diffraction*, 2nd ed. (Addison-Wesley, Reading, MA, 1978).
[26] R. W. Bozorth, *Ferromagnetism* (Van Nostrand, New York, 1951).
[27] J. Du, L. N. Tong, Y. X. Sui, M. Lu, H. W. Zhao, K. Xia, H. R. Zhai, and H. Xia, Z. Phys. B: Condens. Matter **104**, 387 (1997).

[28] A. Kharmouche, J. Ben Youssef, A. Layadi, and S. M. Chrif, J. Appl. Phys. **101**, 113910 (2007).
[29] H. Hashizume, K. Ishuji, J. C. Lang, D. Haskel, G. Srajer, J. Minár, and H. Ebert, Phys. Rev. B **73**, 224416 (2006).
[30] M. T. Johnson, P. J. Bloemen, F. J. den Broeder, and J. J. de Vries, Rep. Prog. Phys. **59**, 1409 (1996).
[31] A. Dinia, K. Ounadjela, A. Arbaoui, G. Suran, D. Muller, and P. Panissod, J. Magn. Magn. Mater. **104-107**, 1871 (1992).